

Density functional study for structure and electronic properties of $\text{FeS}_2(100)$ ^①

QIU Guan-zhou(邱冠周), XIAO Qi(肖奇), HU Yue-hua(胡岳华), QIN Wen-qing(覃文庆)
(School of Resource Processing and Bioengineering, Central South University, Changsha 410083, China)

Abstract: The electronic properties of $\text{FeS}_2(100)$ surface were studied by using a density-functional theory (DFT) method. The very stable (100) surface does not give any significant geometric relaxation and can be regarded as a simple termination of the bulk structure along a plane of cleaved Fe-S bonds. The electronic structure of $\text{FeS}_2(100)$ surface is characterized by surface states in its forbidden zone. The highest occupied and the lowest unoccupied states localize at surface Fe sites. Fe sites are energetically favored over S₂ sites for redox interaction with electron donor or acceptor species on (100) surface.

Key words: density functional theory (DFT); surface energy; electronic structure of surface; native surface state; FeS_2

CLC number: O 472; TD 923

Document code: A

1 INTRODUCTION

The reactivity of the FeS_2 (pyrite) surface is of particular important in the engineering applications, including sulfide minerals flotation^[1], bioleaching of low-grade chalcopyrite-containing ore^[2], coal processing, hydrometallurgy, environmental engineering, geochemistry, and photovoltaic cell, etc^[3]. Especially, an understanding of how pyrite surfaces interact with flotation reagent molecules will aid in the design of more effective flotation suppressants, which would effectively separate the desirable ores from pyrite.

A number of recent experimental studies have been performed on the surfaces of pyrite. Low energy electron diffraction (LEED) and low energy ion scattering results^[4], and scanning-tunneling microscopy (STM)^[5] images indicate that $\text{FeS}_2(100)$ surface prepared via cleaving is essentially unreconstructed. For the clean (100) surface of n - FeS_2 single crystals, the surface electronic structure has been analyzed by photoelectron spectroscopy with different excitation energies^[6] and evaluated on the basis of ligand field theory. According to these results, surface states originate from a symmetry reduction of the Fe coordination at the surface sites. But there are only a few theoretical calculations on the electronic structure of $\text{FeS}_2(100)$ ^[7].

$\text{FeS}_2(100)$ surfaces are known to be cleaved poorly. As a result, (100) surfaces of real FeS_2 samples are likely to have a high density of defects and imperfections such as steps and kinks, which expose

low-coordination (< 5). The aim of the present paper is, by using first-principles calculations, to build up a detailed picture of the energetic, atomic structure and electronic structure of the clean, defect-free stoichiometric $\text{FeS}_2(100)$ surface, which will set up the basis for the study of (100) surface with steps and kinks. The calculations are based on the density-functional pseudo-potential approach, which has already been proved highly successful in many previous studies of oxide surfaces. Our previous work^[8] on the application of density-functional theory (DFT) of the study of bulk pyrite shows that such methods are capable of producing calculated bulk properties such as lattice constants and bulk moduli which agree well with experimental results, and provide a foundation for the present study of pyrite surfaces.

2 METHODOLOGY

In the present study, the Cambridge Serial Total Energy Package (CASTEP) program was used. The theoretical basis of CASTEP is the DFT^[9] in the local density approximation (LDA) or gradient-corrected LDA version, as developed by Perdew^[10] with the application of a pseudo-potential concept. First-principle, norm-conserving pseudo-potentials in Kleinman-Bylander representation were generated using the optimized scheme of Lin et al^[11] in order to reduce the required value of the plane-wave cut-off E_{cut} . The LDA exchange-correlation energy was represented by the Ceperley-Alder formula^[10]. The self-consistent ground state of the system was determined using the

① **Foundation item:** Project (50234010) supported by the National Natural Science Foundation of China

Received date: 2003-01-15; **Accepted date:** 2003-05-28

Correspondence: XIAO Qi, PhD; Tel: +86-731-8830543; E-mail: xiaoqihsp@263.net

Car-Parrinello approach, in which the total energy was minimized with respect to the plane wave coefficients of the occupied orbital.

2.1 Bulk simulation

FeS₂ crystallizes within space group T_h^6 -Pa3 with four formula units FeS₂ per unit cell, as shown in Fig. 1^[12]. Each Fe atom is coordinated to six S atoms in a slightly distorted octahedron, and each S atom is coordinated to three Fe atoms and one S atom in a distorted tetrahedron. The S-S bond is oriented along body diagonals of the cubic cell. A supercell approach was used by applying the three-dimensional periodic boundary condition to the FeS₂ unit cell. The structural properties of bulk FeS₂ were investigated by calculating the total energy for the unit cell as a function of the lattice parameter a_0 and of the Wyckoff parameter u .

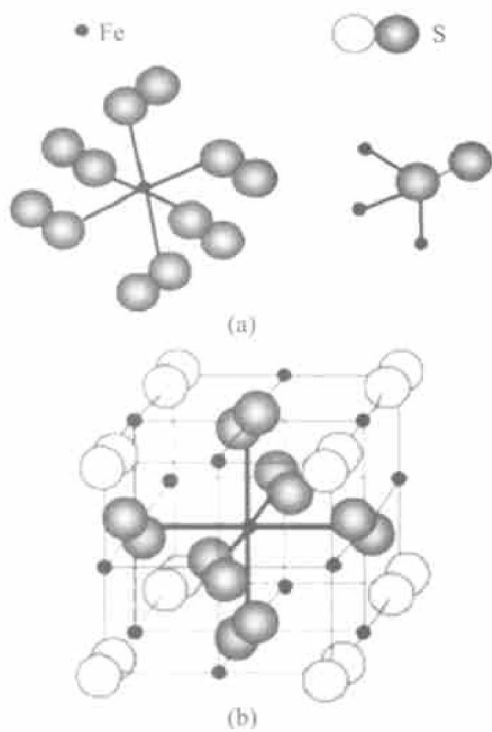


Fig. 1 Bulk FeS₂ unit cell

2.2 Surface models

A general view of the stoichiometric (100) surface of FeS₂ is shown in Fig. 2. This surface termination was suggested by a recent STM study of FeS₂ (100)^[5]. The terminology of the (100) surface structure is as follows. The (100) surface where no S₂ pair is broken and that keeps the S-Fe-S triple layer intact is by far the stablest and is the one to be considered here. With this choice of the surface plane position, the surface atom is a sulfur one. This atom has a sulfur atom and two iron atoms as neighbors and is only missing one Fe neighbor compared with the situation in the bulk. The Fe atom just below is bonded to five S₂ pairs instead of six for the bulk.

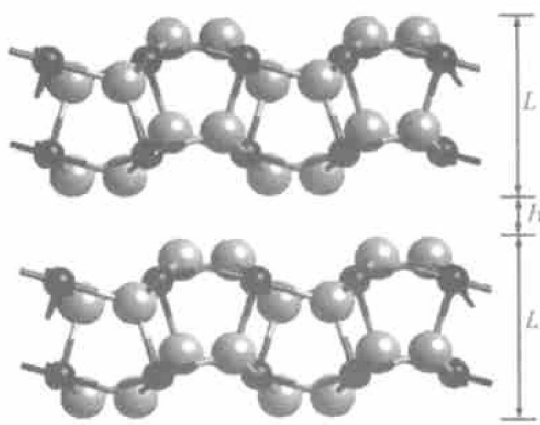


Fig. 2 Perspective view of stoichiometric FeS₂(100) surface (small dark spheres and large light spheres represent Fe and S, respectively)

Our surface calculations work with infinite slabs of material. Because three-dimensional periodic boundary conditions were used, the calculations are actually performed on an infinite stack of slabs, with each slab separated from its neighbors by a vacuum layer, assuming that both slab thickness L and vacuum width H are large enough to make the interaction between surfaces negligible.

3 RESULTS AND DISCUSSION

3.1 Crystalline and electronic structure of bulk FeS₂

The optimum parameters from the calculation are listed in Table 1. The results are in excellent agreement with the experimental data^[12]. The calculations of the electronic structure are conducted using the experimental lattice parameters.

The calculated density of states for FeS₂ is

Table 1 Summary of geometry optimization for FeS₂

Item	a_0 /nm	u	d_{SS} /nm	d_{FeS} /nm
Theoretical	0.538 23	0.384 56	0.214 4	0.224 9
Experimental ^[12]	0.541 6	0.385	0.216 2	0.226 9
Deviation (%)	-0.6	-0.2	-0.2	-0.9

presented in Fig. 3. These results are very similar to the number of published calculations for FeS₂ (pyrite)^[13] and in excellent accordance with the experimental data^[14]. It can be described in terms of states of S₂²⁻ molecular ions (3sσ, 3sσ*, 3pσ, 3pπ and 3pσ*) and of crystal-field split 3d states of Fe²⁺ (e_g and t_{2g}). The lowest two bands near -20 eV and -10 eV are well described by the bonding and antibonding of molecular states 3sσ and 3sσ*. The band of states between -8 eV and -1 eV can be described

as mixed states derived from molecular states 3p σ , 3p π , 3p π^* and a small part of bonding of the Fe 3d e_g state. The narrow band just below the Fermi level is primarily the nonbonding Fe 3d t_{2g} state. Finally, the unoccupied band above the Fermi levels corresponds to the mixture of the antibonding 3p σ^* state and the Fe 3d e_g states.

3.2 Geometric structure of FeS₂(100) surface

The effect of vacuum width and slab thickness on the surface energy σ was investigated. The surface energy σ is obtained by subtracting the energy of the corresponding number of formula units in the perfect crystal from the energy of the slab, and dividing the result by the total surface area.

Our calculated unrelaxed and relaxed surface energies for the unreconstructed (100) surface are listed in Table 2. It is clear from these results that slabs containing nine layers of ions ($L = 0.8124$ nm) and a vacuum width equivalent to six layers ($H = 1.0832$ nm) give an excellent representation of the semi-infinite crystal with a simple surface. Moreover, surface energy of relaxed surface is only slightly different from that of unrelaxed surface. Collectively, the LEED^[4], STM^[5] and our theoretical results suggest that the (100) surface atomic structure can be regarded as a simple termination of the bulk, and there is no significant relaxation.

Table 2 Calculated surface energy of a series of periodic slab systems of different slab thickness L and vacuum width H

(100) surface	L / nm	H / nm	Surface energy / ($J \cdot m^{-2}$)
Unrelaxed surface	0.5416	0.2708	1.3500
	0.5416	0.5416	1.2460
	0.5416	0.8124	1.2430
	0.5416	1.0832	1.2428
	0.8124	1.0832	1.2395
	1.0832	1.0832	1.2390
Relaxed surface	0.8124	1.0832	1.2300

3.3 Electronic structure of (100) surface

The calculated total density of states (DOS) of the unrelaxed nine-layer slab is compared with the bulk DOS obtained in our earlier work^[8] in Fig. 4. There are three important differences. Firstly, there is a slight reduction in the width of the gap. The calculated gap for the bulk is 0.65 eV, while for the nine-layers slab system the gap is about 0.16 eV. Secondly, our theoretical results of the slabs exhibit

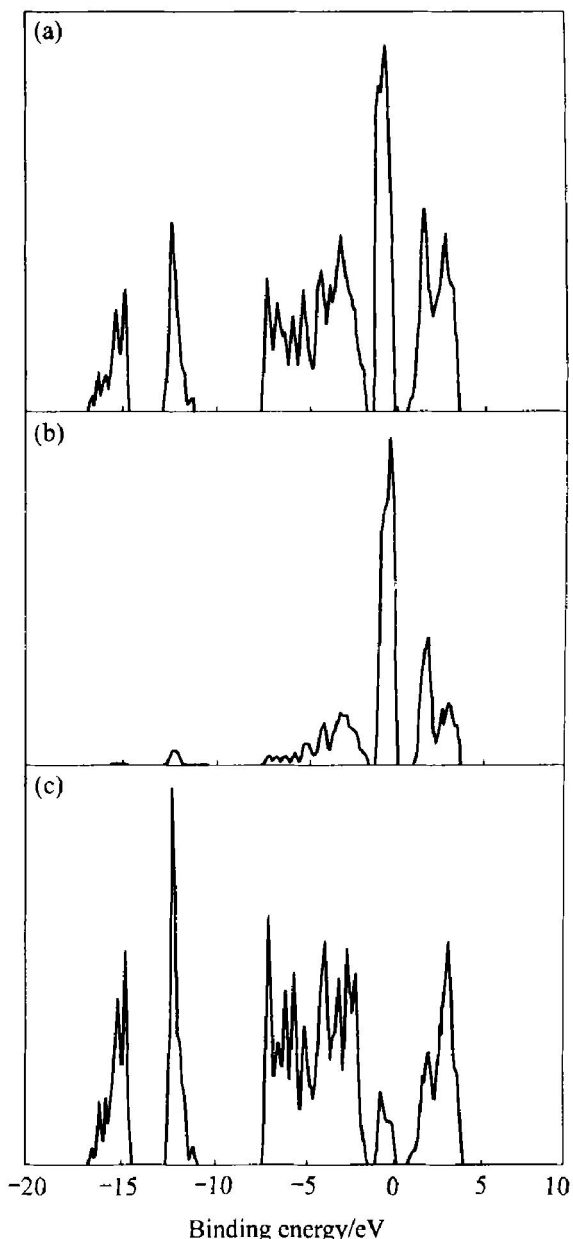


Fig. 3 Calculated density of states for perfect FeS₂ crystal

(a) —Total density of states;
(b) —Local density of states for Fe atom;
(c) —Local density of states for S atom

new electronic states F_1 in the gap. Thirdly, that in the slab system, a new state F_2 exists in the energy range from -1 eV to -3.5 eV.

In order to understand the above-mentioned results, the partial density of states of (100) slab was calculated. Figs. 5(a)–(c) show the DOS of Fe 3d, Fe 4p and S 3p, respectively. In the gap, there exists a higher peak of DOS arising from Fe 3d compared with DOS of Fe 3p and S 3p. This indicates that the new surface state F_1 in the gap primarily originates from Fe 3d state. In the energy range from -1 eV to -3.5 eV, the DOS of Fe 3d and S 3p have nearly the same peaks. This means that there is a significant hybridization between Fe 3d and S 3p and the surface state F_2 originates from the hybridization between Fe

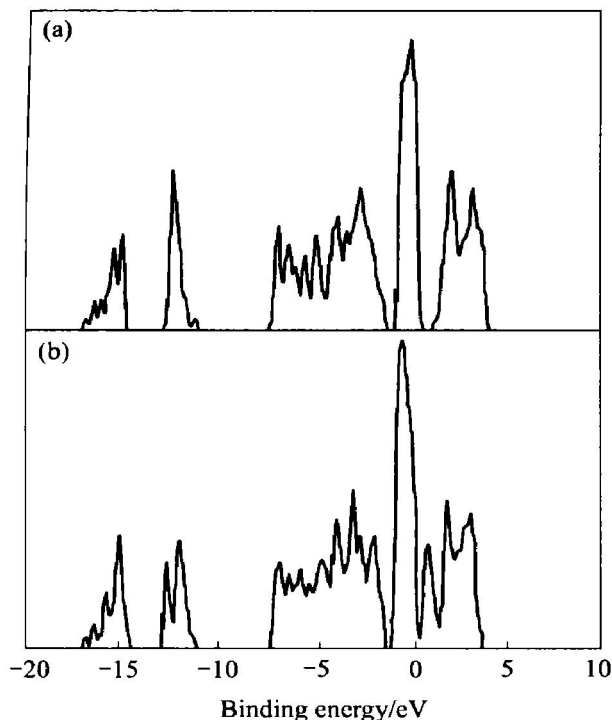


Fig. 4 Total density of states for perfect crystal(a) and nine-layer stoichiometric slab(b)

3d and S 3p.

Now, with the band structure model for pyrite with a sulfur deficit developed by Birkholz et al^[15], the origin of surface states was discussed from the perspective of ligand-field theory (LFT) (Fig. 6). In the FeS_2 bulk, Fe 3d states are split into t_{2g} and e_g levels in an octahedral ligand field. At the (100) surface, the loss of one S ligand leads to a square pyramidal field around the Fe atoms and energetically destabilizes every Fe 3d orbital with a Z component (Z arbitrarily chosen normal to the surface plane). This effect is primarily seen in the splitting of e_g states, with the so-called Fe *a* state having a lower energy. The *a* states combine with S sp^3 states to form bonding states (σ defect states) and antibonding states (σ^* defect states) which correspond to the new surface states F_2 and F_1 , respectively.

According to the above calculation results, Fe 3d t_{2g} states and F_1 states construct the highest occupied molecular orbital (HOMO) and the lowest unoccupied molecular orbital (LUMO) at the surface, respectively. In fact, STM images and STS also indicate that both the HOMO and LUMO are located at the surface Fe sites. So, Fe sites are energetically favored over S₂ sites for the interaction with electron donor or acceptor species on (100) surface. In the following papers written by the authors, the interaction of (100) surface with flotation reagent molecules mixtures will be discussed in order to further investigate and design novel reagent used in flotation

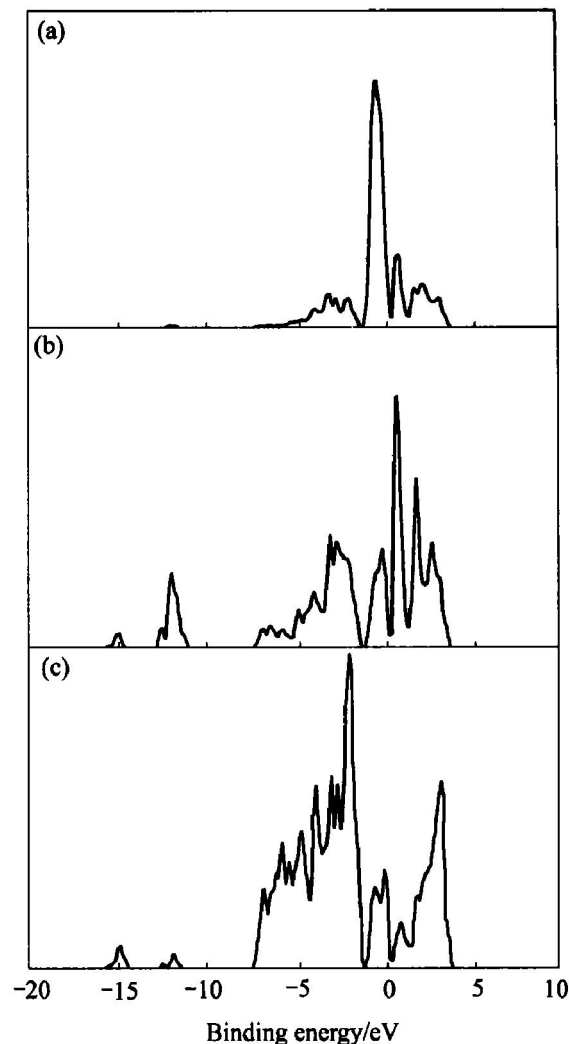


Fig. 5 Calculated projected densities of states for Fe 3d(a), Fe 4p(b) and S 3p(c) states in (100) surface environments

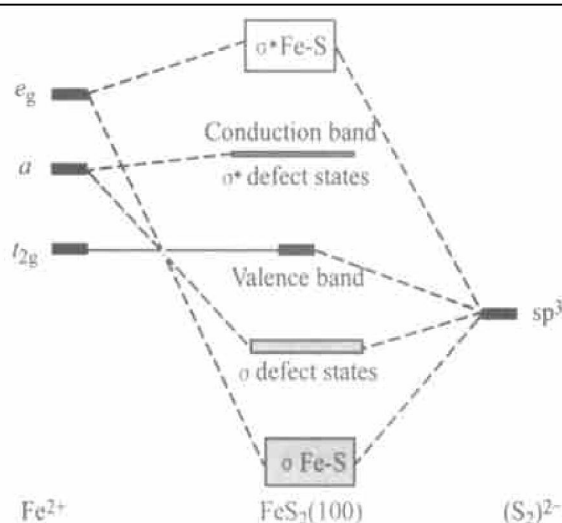


Fig. 6 Most prominent features of electronic structure model for $\text{FeS}_2(100)$

environments.

4 CONCLUSIONS

The (100) surface does not give any significant geometric relaxation and can be regarded as a simple termination of the bulk structure along a plane of the cleaved Fe–S bonds, while the electronic structure of FeS₂(100) surface is characterized by new surface states in the forbidden zone. Both the HOMO and the LUMO are located at the surface Fe sites. So, Fe sites are energetically favored over S₂ sites for redox interaction with electron donor or acceptor species on (100) surface.

ACKNOWLEDGEMENTS

Helpful discussion with Professor WANG Dianzuo and Professor YU Zhirming are gratefully acknowledged.

REFERENCES

- [1] HU Yuehua, QIU Guangzhou, SUN Shuryu, et al. Recent development in researches of electrochemistry of sulfide flotation at Central South University of Technology[J]. Trans Nonferrous Met Soc China, 2000, 10(S) : 1 – 7.
- [2] QIU Guangzhou, WANG Jun, HU Yuehua, et al. Bio-leaching of low-grade large porphyry chalcopyrite-containing ore[J]. Trans Nonferrous Met Soc China, 2000, 10(S) : 19 – 22.
- [3] Ennaoui A, Fiechter S, Pettenkofer C, et al. Iron disulfide for solar energy conversion[J]. Solar Energy Materials and Solar Cells, 1993, 29: 289 – 292.
- [4] Jaegermann P W, Bronold M. Site specific surface interaction of electron donors and acceptors on FeS₂(100) cleavage planes[J]. Ber Bunsenges Phys Chem, 1991, 95 (5) : 560 – 565.
- [5] Siebert D, Stocker W. Investigation of a (100) surface of pyrite by STM[J]. Phys Stat Sol A, 1992, 134: 17 – 21.
- [6] Bronold M, Tomm Y, Jaegermann W. Surface states on cubic d-band semiconductor pyrite(FeS₂) [J]. Surf Sci Lett, 1994, 314: 931 – 936.
- [7] WANG Dianzuo, LONG Xiangyun, SUN Shuryu. Quantum chemical mechanism on the surface oxidation and flotation of sulfide minerals[J]. The Chinese Journal of Nonferrous Metals, 1991, 1(1): 15 – 23. (in Chinese)
- [8] QIU Guangzhou, XIAO Qi, HU Yuehua, et al. Density functional calculation of equilibrium geometry and electronic structure of pyrite[J]. Trans Nonferrous Met Soc China, 2001, 11(4) : 583 – 586.
- [9] Kohn W, Sham L J. Self-consistent equations including exchange and correlation effects[J]. Physical Review A, 1965, 140(4) : 1133 – 1138.
- [10] Perdew J P, Zunger A. Self-interaction to density-functional approximations for many-electron systems [J]. Physical Review B, 1981, 23(10) : 5048 – 5079.
- [11] Lin J S, Qteish A, Payne M C, et al. Optimized and transferable nonlocal separable ab initio pseudopotentials [J]. Physical Review B, 1993, 47(8) : 4174 – 4180.
- [12] Vaughan D J, Craig J R. Mineral Chemistry of Metal Sulfide [M]. London: Cambridge University Press, 1978.
- [13] Opahle I, Koepernik K, Schrig H E. Full-potential band structure calculation of iron pyrite[J]. Physical Review B, 1999, 60(20) : 14035 – 14041.
- [14] van der Heide H, Hemmel R, van Bruggen C F, et al. X-ray photoelectron spectra of 3d transition metal pyrites[J]. Journal of Solid State Chemistry, 1980, 33 (1): 17 – 25.
- [15] Birkholz M, Fiechter S, Hartmann A, et al. Sulfur deficiency in iron pyrite(FeS_{2-x}) and its consequences for band structure models[J]. Physical Review B, 1991, 43(14) : 11926 – 11936.

(Edited by LI Xiangqun)